ChemCatChem

Research Article
doi.org/10.1002/cctc.202301015

Chemistry Europe
European Chemical Societies Publishing

www.chemcatchem.org

$H_2[Pt(C_2O_4)_2]$ as a Tailor-made Halide-free Precursor for the Preparation of Diesel Oxidation Catalysts: Nanoparticles Formation, Thermal Stability and Catalytic Performance

F. Spolaore,[a, b] C. Hengst,[a] F. Dornhaus,[a] M. Votsmeier,[a, c] and S. Gross*[b, d]

The aim of this study was to investigate a tailor-made metal precursor and its chemical properties to tune the properties of supported metal nanoparticles (NPs) and their catalytic performance when used as Diesel Oxidation Catalyst (DOC). The formation of extremely small Pt NPs from a new halide-free Pt complex was investigated, namely bis(oxalato)platinate, $H_2[Pt(C_2O_4)_2]$. The size evolution of the supported NPs, from the formation upon the Pt precursor decomposition on γ-alumina to the sintering of the NPs at high temperatures, was followed by thermogravimetric analysis coupled with mass spectrometry (TG-MS) and differential scanning calorimetry (DSC), transmission electron microscopy (TEM) and diffuse reflectance infrared Fourier transform (DRIFT) spectroscopy. A correlation between the NPs' size of the catalyst and the performance for the CO, C_3H_6, C_3H_8 and NO oxidation reactions pointed out a retained activity during test cycles, showing low sensitivity to the test conditions applied (i.e., temperature and gas composition). The overall catalytic performance was better in the fresh catalysts compared to the reference catalyst prepared from platinum nitrate, $Pt(NO_3)_4$. In particular, the different dispersion of the Pt NPs over the support obtained from the two precursors was identified as the reason for the different catalytic performance, retaining small NPs size after the tests cycles.

Introduction

Environmental and health concerns pushed in the past decades the vehicle market to adopt effective exhaust gas aftertreatment systems, subject of a broad number of reviews.[1–4] The optimisation of such systems, aiming to maximise the conversion of the exhaust gases, prompted the research for the best compromise between size (surface area), shape (selectivity) and stability (against sintering) of the precious metal active components.[5–7] Some catalysed reactions were indeed found to display a volcano behaviour, with small NPs leading to lower catalytic performance despite the exponential increase of specific surface area.[8,9]

Additionally, the smaller the metal NPs, the lower the stability towards temperature, and the easier they undergo sintering when exposed to the often harsh conditions occurring during their use as catalysts, leading to an abrupt increase in particle size and often to dramatic loss in catalytic performance.[10–12]

Two competing mechanisms were proposed to describe the loss of performance due to the thermal sintering: the Ostwald ripening and the particle migration and coalescence.[13] The relative magnitude of both mechanisms is dependent, among other factors, to the type of metal, the temperature and the initial size of the NPs. Consequently, the initial size distribution affects the stability of the catalyst and the subsequent size broadening of the constituting NPs when temperature rises, which is the main factor determining the degree of motion over the support and the specific vapor pressure that reduce the active surface area.[14]

Pt/Al_2O_3 is a model catalyst for DOC to study impact of preparation and pre-treatment procedures, metal-support interaction or impact of testing gas composition, whereas state of the art Diesel automotive catalyst includes also Pd for its ability to improve the durability of the catalyst.[15–18] Indeed, the catalyst deactivation is still nowadays subject of investigation both in academia and in industry.[4] Beside high operating temperatures, deactivation can arise from chemical poisoning ascribed to impurities such as Na, K, Ca, P or S.[19,20] Alongside such impurities, halides are known to deactivate the active metals of the catalysts for certain oxidation reactions.[21] The choice of Pt metal precursor for catalyst heterogeneous

[a] Dr. F. Spolaore, Dr. C. Hengst, Dr. F. Dornhaus, Prof. M. Votsmeier
Automotive Department
Umicore AG & Co. KG
Rodenbacher Chaussee 4, 63457, Hanau (Germany)

[b] Dr. F. Spolaore, Prof. S. Gross
Department of Chemical Sciences
University of Padova
via F. Marzolo 1, 35131 Padova (Italy)
E-mail: silvia.gross@unipd.it

[c] Prof. M. Votsmeier
Chemistry Department
TU Darmstadt
Alarich-Weiss-Str. 8, 64287 Darmstadt (Germany)

[d] Prof. S. Gross
Institute for Chemical Technology and Polymer Chemistry (ITCP)
Karlsruhe Institute of Technology (KIT)
Engesserstr. 20, 76131 Karlsruhe (Germany)

Supporting information for this article is available on the WWW under https://doi.org/10.1002/cctc.202301015

preparation is therefore important and the most widely used Pt salt solutions for are the following:, $Pt(NO_3)_4$,[22] $Pt(NO_3)_2$,[23,24] $Pt(NH_3)_4$,[25] $Pt(NH_3)_4(ac)_2$,[26] $Pt(NH_3)_4(NO_3)_2$,[27,24] $(NH_4)_2PtCl_4$,[26] $Pt(NH_3)_4Cl_2$,[28] $Pt(NH_3)_4(OH)_2$,[29] $Pt(acac)_2$[30] and of course the well-known $H_2Pt(Cl)_6$.[31] The effects of these different Pt precursors on catalytic performances for various reactions is a research subject of interest, with contradictory rankings depending on the investigated reactions and their specific structure-sensitivity.[29,31,32] Halide-free Pt precursors are reported to generate smaller NPs, particularly those containing amine groups. The catalysts prepared from $Pt(NH_3)_4(NO_3)_2$ and $Pt(NH_3)_4(Ac)_2$ showed in previous studies higher Pt dispersion and smaller Pt particles size compared with halide containing $(NH_4)_2PtCl_4$, and H_2PtCl_6.[26] Moreover, metal loss through formation of volatile compounds (e.g., halides) is generally recognized as a significant route to catalyst deactivation.[21] The presence of halides (e.g., chloride) affects sintering and redispersion by increasing the metal atom mobility on the support, forming volatile chlorides of the active metal, followed by gas-phase transport from the support. Additionally, halides can induce changes in the oxidation state thereby impacting the reactivity of the active metal NPs.[33] Pt catalysts are indeed known to be sensitive to chlorine, with Pt NPs undergoing reconstruction under reaction conditions starting at about 600 °C, leading to the formation of large faceted metal particles. Moreover, even after calcinations and reductions, chlorine tends to remain on the alumina based catalysts, acting as an inhibiting species for hydrocarbons oxidation.[34] The impact of the chlorine amount, introduced with the metallic precursor (H_2PtCl_6), and its inhibition on the activity for Pt catalysts was investigated by Marceau et al.[35] For these reasons, one of the most common Pt precursor for automotive catalysts is the halide-free Pt(IV) nitrate one.[22]

Despite years of research, it is still extremely difficult to stabilize the catalytically active Pt sites on supports in order to extend the life-time of working catalysts. Since CO inhibits the oxidation of HCs and NO, their light-off is observed only after CO is fully converted. Therefore, a challenge today is to develop catalysts that could display CO and HCs light-off below 150 °C after aging.[1] Among the different strategies, maximizing the Pt dispersion over the support was proposed as one way to limit the formation of 'anomalously' large Pt particles after aging in air at temperatures above 600 °C.

In the pursue of preparing a more stable catalyst, through enhanced Pt dispersion over the support, a not yet reported halide-free Pt precursor, namely bis(oxalato)platinate, $H_2[Pt(C_2O_4)_2]$, was tested and cross-referenced with Pt nitrate. The $H_2[Pt(C_2O_4)_2]$ complex was synthesised for the first time over 190 years ago by Döbereiner,[36] investigated later on by Söderbaum[37,38] and by Krogmann and Dodel[39,40] in 1969. To the best of our knowledge, there are no previous reports where this precursor has been used as metal precursor for the synthesis of supported Pt NPs, particularly at the kg scale. There are previous studies where this precursor was applied for the synthesis of Pt colloidal NPs in water with hydrogen in the presence of oxalate as a stabilizing agent.[41]

The physico-chemical properties of the bis(oxalato)platinate are peculiar: this complex is indeed characterised by a dynamic and highly complex aqueous chemistry, forming dimers and units of higher molecular complexity. These oligomers were investigated in solution by means of ^{195}Pt-NMR[42] and, as isolated crystals, by X-ray analysis,[43] and the formation of long needle-like crystals constituted by many Pt monomeric units arranged in solution was proposed.[44,45] This behaviour, coupled with the high exothermic decomposition of the oxalate ligands, was exploited in this work to enhance the dispersion of the Pt NPs over the selected metal oxide support γ-alumina. A correlation between the physical properties of the NPs obtained from the two Pt precursors and the chemical performances for CO, hydrocarbons (HCs) and NO oxidation was then assessed after different thermal treatments.

Results and Discussion

Prior to the deposition on γ-alumina, differently concentrated Pt salt solutions were characterised by UV-Vis to assess the state of the precursor mimicking the synthetic conditions for the catalysts' preparation. The UV-Vis analysis were performed on increasingly diluted solutions, quickly moving from bigger oligomers (in concentrated solutions) to smaller ones (in diluted solutions). The study was performed indeed to characterize the state of the Pt complex solution used during the synthesis of the Pt NPs, that led to the formation of small and highly uniform NPs of about 1–2 nm, to exclude the possibility that size variations were induced by the formation of notably different species. Indeed, the UV-Vis analysis of the $H_2[Pt(C_2O_4)_2]$ solution (Figure S1) displayed the peculiar behaviour previously observed by Krogmann[39,40] and Keller,[46] namely a concentration dependence of the UV-Vis absorption maxima associated to the presence of different oligomers in solution.[42,43] Their presence was confirmed also by ATR spectroscopy (Figure S2) and the relative ratio of the different oligomers was found to depend both on pH and on concentration,[42] with more concentrated and acidic solutions containing structures with higher degree of polymerisation, a trend that was also observed in the present study (Table 1). Assignment of the bands was performed based of literature data[46] and the Pt complexes with relative absorption maxima are listed in Table S1. As previously reported, at least four distinct maxima in the solutions absorption spectra were found at $\lambda_{max} = 426$, 510, 600 and 680 nm varying the Pt concentration. Keller et al. attributed

Table 1. List of UV-Vis absorption peaks of bis(oxalato)platinate solutions analysed in this work at different c Pt [mol/L].

Sample	c Pt [mol/L]	Absorption peak maxima [nm]
a	0.60	260, 328, 381, 510, 600, 680, 1000.
b	0.15	260, 378, 510, 660, 945.
c	0.10	260, 328, 510, 600, 680.
d	0.02	260, 378, 424.

these UV-Vis absorption bands to a series of oligomers and confirmed the structures with ^{195}Pt-NMR.[46] Given the sensitivity of the Pt precursor to the dilution applied during the preparation of the NPs (Table 1), the UV-Vis study showed that this precursor contained mainly complexes with a low degree of polymerisation when employed at 0.02 mol/L, namely monomers and dimers. During the preparation of the supported NPs, a thermal treatment in air of the precursor impregnated on γ-alumina was applied, leading to the degradation of the precursor. As pointed out from the TG-MS coupled with DSC analysis (Figure S3), the decomposition of such complex starts at 170 °C, as evidenced by the evolution of CO_2 (Figure S4). Using a diluted (0.02 mol/L) Pt precursor, the preparation of catalysts was then optimised to maximise the dispersion: first, a screening of the synthetic parameters was performed, followed by a thermal stability study to ensure stable and long-lasting catalysts and consistent catalytic test results. Initially, selected synthetic parameters for the preparation of the catalysts were modified assessing changes in particle size and catalytic performance.[47] Three different factors were varied: i) temperature (25 °C–70 °C), ii) time of impregnation (15 min–60 min) and iii) initial Pt concentration with respect to the alumina support (1–10 wt% Pt). The samples were first dried at 350 °C/15 min, then calcined at 550 °C/2 h prior to the tests and the total amount of Pt was measured by ICP-OES and normalized with alumina for the catalytic tests. The particle size of the prepared catalysts was analysed by means of CO chemisorption analysis (Table S2), assuming spherical particles. Despite varying these three factors, all catalysts displayed an average size between 2.3 and 3.2 nm. The light-off temperature for the CO oxidation reaction (sensitive tool to indirectly evaluate the NPs size) was used to confirm this result. Smaller NPs would indeed display a lower light-off temperature, i.e. a higher catalytic performance. The observed light-off temperatures indeed correlate well with the CO absorption tests, meaning that all synthetic conditions resulted in highly dispersed NPs over the alumina support, with no significant changes (10 K span among all curves, Figure S5). The most efficient synthetic condition was selected (i.e., 1 wt% Pt, 25 °C and 15 min impregnation) and with this set of reaction parameters one additional factor was investigated, namely the pH. Known to affect the speciation and equilibria in solution of bis(oxalato)platinate precursor,[43,44] this parameter was separately investigated. A washcoat containing γ-alumina impregnated with bis(oxalato)platinate was prepared and at this stage the pH was varied (aiming at two different pH target values, i.e., pH 2 and 6) with two different acids (oxalic acid and nitric acid, see the Experimental Section for preparation details). These four washcoats were then coated on cordierite monoliths and tested for the oxidation of CO, HCs, and NO. In both fresh (Figure S7, A-B-C) and aged samples (Figure S7, D-E-F) and for all oxidation reactions, one particular sample (pH = 2 with addition of oxalic acid) outperformed the others, displaying a lower light-off temperature and higher catalytic performance. As possible explanation, the impregnation on the alumina at acidic pH with free oxalic acid likely influenced the degree of oligomerisation during the adsorption process, as observed by the appearance of an intense blue colour for this particular washcoat. Moreover, Dou et al., also suggest that Pt nitrate complexes chemisorb more efficiently on alumina than the monomers and dimers of diluted solutions of Pt-oxalate (coherent with the UV-Vis trend observed).[48] The resulting Pt oxalate complexes decompose faster and at lower temperature compared to the nitrate ones, leaving less room for migration phenomena that would instead lead to growth of the Pt particles.[13] The thermal stability of the supported Pt NPs for this particular sample were then investigated by means of TEM and DRIFT spectroscopy. Figure 1 and Table 2 show the NPs and the respective average particle sizes after treating the samples at different temperatures in ambient air. As a result of the sintering process occurring at increasingly higher temperatures, the NPs were expected to rapidly increase in size. Surprisingly, the starting NPs did not significantly alter their

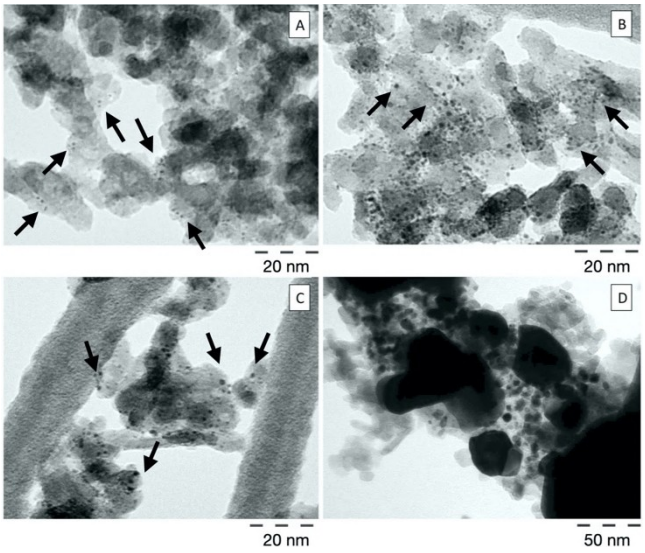

Figure 1. TEM pictures of Pt NPs on γ-alumina (1 wt%) from bis(oxalato)platinate, after different thermal treatments: 350 °C/15 min (sample A), 350 °C/4 h (sample B), 550 °C/2 h (sample C) and 800 °C/16 h (sample D).

Table 2. Average particle sizes obtained by TEM, calculated specific active surface area and range distribution for 1 wt% Pt containing γ-alumina, treated at different temperatures.

Samples	dn[a] nm	ds[a] nm	dv[a] nm	Specific surface area[b] m^2/g	D90[c] nm
Sample A 350 °C/15 min	0.6	0.6	0.7	434	0.4–0.9
Sample B 350 °C/4 h	0.7	0.7	0.8	377	0.5–1.0
Sample C 550 °C/2 h	0.8	0.9	1.0	312	0.6–1.4
Sample D 800 °C/16 h	20.1	64	98	4.4	6.5–33.9

[a] average number (n), surface (s) and volume (v) particle diameters. At least 1000 counts for each sample were done, beside for sample D with 100 counts. [b] calculated specific surface area assuming spherical NPs. [c] range distribution of 90% number count based particles.

average particle size and remained below 1 nm in D90, and preserved a sharp size distribution even after 550 °C/2 h.

Finally, when exposed to a harsh aging process used to simulate the catalyst aging (800 °C/16 h hydrothermal, Figure 1 D) the Pt particle size rapidly increased, reaching a mean size of about 20 nm and broad distribution. DRIFT spectroscopy (Figure 2) confirmed the spatially localised observations made by TEM. Indeed, changes in particle size are expected to impact the stretching signals of CO bonded on Pt.[49,50] It is generally agreed that CO adsorbs on this metal linearly, with an almost pure 180° degree coordination geometry, and that the bands located between 2000 and 2100 cm^{-1} are assigned to the stretching of CO molecules adsorbed on Pt atop sites, the 1950–1850 cm^{-1} to bridge sites and the ones at 1800–1650 cm^{-1} to hollow sites.[51] Further assignments of the stretching of CO molecules linearly adsorbed on Pt atop sites were proposed by Garnier et al.[52] They attributed three infrared bands with decreasing absorption frequencies to an adsorbed CO molecule, whether it is linearly adsorbed onto faces, edges, and corners surface sites of a particle: these sites contribute to frequencies of about 2096, 2083 and 2072 cm^{-1}, respectively. In addition, an even lower adsorption wavelength was proposed, corresponding to multiple CO adsorptions on a single Pt corner site, characterised by an IR absorption at about 2054 cm^{-1}. Casapu et al. also characterized differently sized Pt/Al_2O_3 catalysts by DRIFT spectroscopy during the CO adsorption and desorption at different temperatures and observed that very small Pt display a stronger adsorption of CO on small NPs (below 1.5 nm).[53] The appearance of high wavenumbers signals became predominant for larger Pt NPs (above 5 nm) obtained with aged Pt/Al_2O_3 catalyst. In addition, the group reported that the adsorption of CO follows different paths depending on the Pt particle size. For NPs between 1–2 nm, CO was proposed to initially adsorb at low-coordinated/corner Pt sites (2059 cm^{-1}), and only at higher CO coverage the terrace sites (2079 cm^{-1}) are filled. Such observations are in agreement with the Density functional theory (DFT) calculations by Li et al., that observed that adsorption energies of CO and O depend on the size of Pt NPs and significantly change for Pt NPs below 1.6 nm, resulting in lower adsorption wavelengths.[54]

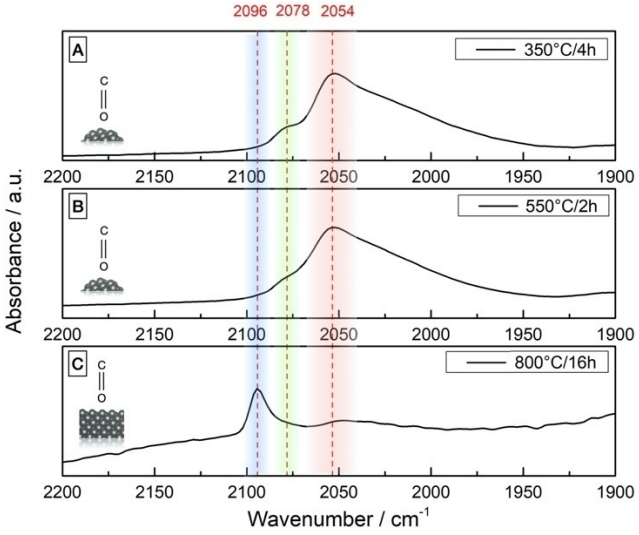

Figure 2. DRIFT spectra of chemisorbed CO on the same 1 wt% Pt sample (TEM in Figure 1) after three different thermal treatment. From top to bottom, degreened (350 °C/4 h), calcined fresh (350 °C/4 h + 550 °C/2 h) and aged (350 °C/4 h + 550 °C/2 h + 800 °C/16 h).

These corner sites are particularly abundant in very small NPs,[55] as confirmed by our results. Indeed, Figure 2 (A–B) shows the assignments of the CO absorption peaks at 2078–2054 cm^{-1}, and 1840 cm^{-1} (Figure S8 for the full spectra), relative to linear and bridged adsorbed CO, respectively. DRIFT spectroscopic studies hence allowed us to follow the evolution of the CO stretching frequency adsorbed on Pt particles during the NPs size evolution from few nm to dozens upon heating. The observed frequencies presented a shift of CO stretching frequencies on atop sites on small NPs (Figure 2A and 2B) that shifted towards lower wavenumbers for CO adsorbed on atop sites of bigger Pt NPs in the order of 15–20 nm (Figure 2C, sample characterised by TEM in Figure 1). This blue-shift from 2050 to 2095 cm^{-1} in frequencies observed was ascribed to the reconstruction of the Pt surface and varying ratio of different adsorption sites.[56] This observation is coherent with the increase in size of the Pt NPs revealed by TEM. When NPs are below 1 nm, they present a relative high number of multiple corners, corners and edges atoms with respect to flat surfaces atoms.[52] The optimised catalyst was then tested as DOC. To evaluate the performance of this catalyst, a reference catalyst was prepared from a Pt-nitrate precursor, kindly provided by Umicore. The two catalysts were then tested both fresh (350 °C/4 h + 550 °C/2 h) and aged (350 °C/4 h + 550 °C/2 h + 800 °C/16 h). The catalytic performance was tested for standard DOC pollutants, namely CO, HCs and NO.[10,57] In the fresh state, displayed in Figure 3A-B-C, slightly lower light-up temperatures (about 15 K in T50 for CO, 5 K for T40 for HCs and 4 K for T 30 for NO) and higher total conversions (for CO and NO in particular) were obtained for the bis(oxalato)platinate based catalyst. Such values refer to the third light off, but the same trend was observed in all cycles and the comparison is displayed in Figure 4. Moreover, the test was repeated twice: two different cores were indeed tested a second time confirming the observed trend, with values close to identical absolute values. To explain the observed higher performance for the bis(oxalato)platinate catalyst with respect to the platinum nitrate based one, TEM analysis was carried out on the coated washcoats, both before and after the catalytic cycles. Size distribution histograms of fresh catalysts before and after the test are reported in Figure 5. Surprisingly, the bis(oxalato)platinate based catalyst appeared less sensitive to the applied test conditions (temperature ramp and gas atmosphere), resulting in a smaller gap between the size distribution of fresh not-tested and fresh tested (Figure 5A–B) samples.

All catalysts were degreened and calcined at 350 °C/4 h and 550 °C/2 h in air, so the quick temperature ramp 15 K/min up to 500 °C applied during the three subsequent test cycles was not expected to impact the particle size. The Pt nitrate based catalyst increased the particle size to a higher extent during testing, likely resulting in a lower active specific surface area.

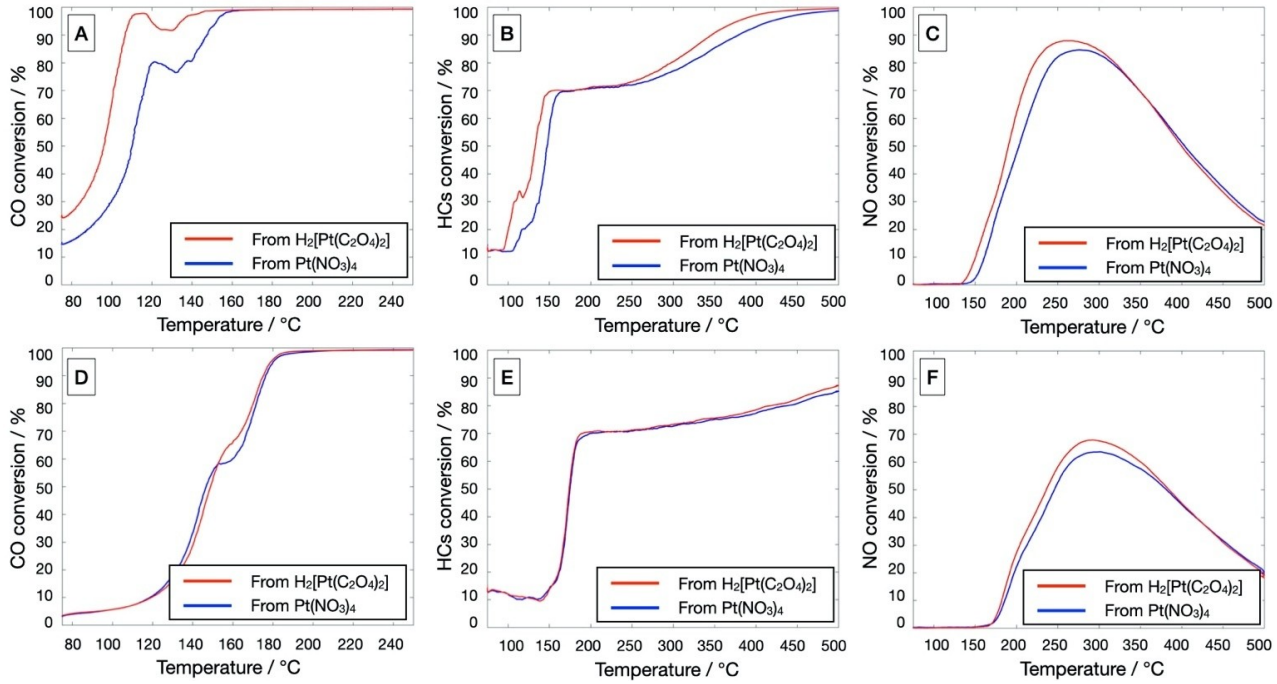

Figure 3. Comparison of the third catalytic light-off between of a bis(oxalato)platinate at pH = 2 and platinum nitrate based catalysts for the oxidation of CO (A–D), HCs (B–E) and NO (C–F). (A, B, C) fresh 550 °C/2 h and (D, E, F) aged 800 °C/16 h.

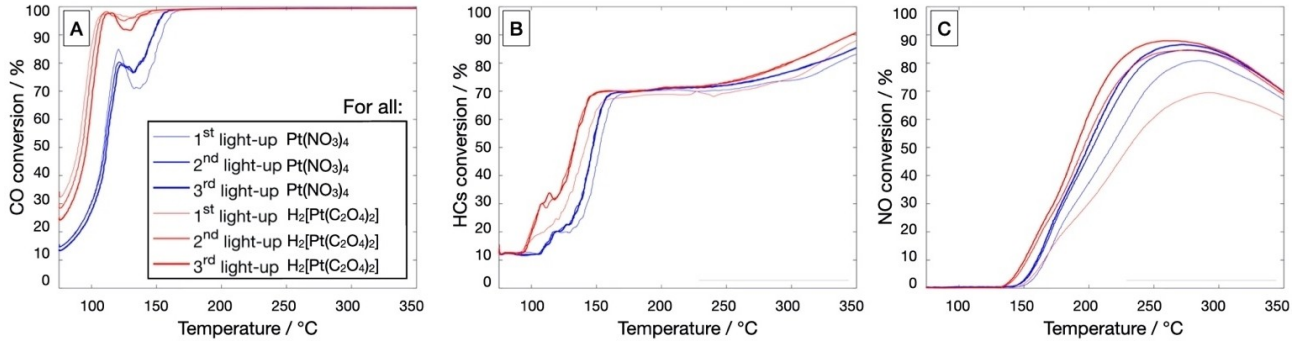

Figure 4. Three subsequent catalytic light-up for CO (A), HCs (B), NO oxidation (C) for (red) Pt oxalato and (blue) Pt nitrate based catalysts. Catalysts consisted of 1 wt% Pt on γ-alumina samples produced by thermal decomposition of impregnated Pt precursors and calcined at 550 °C/2 h.

Indeed, the size increase observed by TEM correlates well with the catalytic performance for the two catalysts, with bigger particles displaying lower performance, in agreement with data reported in literature for similar Pt supported alumina systems.[12] The reconstruction of surfaces under gas atmosphere in the presence of reactants (i.e., CO), the increasing temperature of the test (from 75 up to 500 °C in 1 h test cycle), the repeated test cycles (3 times), a higher water amount with respect the pre-treatment (performed in ambient air) or the exothermic catalysed reactions producing on-spot heat (e.g., CO oxidation), were ascribed as possible reasons for the increase in active particle size for both catalysts.[58,59] Another explanation recently proposed is linked to the Al^{3+} sites of the alumina that could partially bury the active Pt during the oxidation reactions.[60]

As depicted in Figure 4, a shift in the CO light-off temperature of about 3 K with respect to the previous runs was observed. The catalytic performance changes with a regression in the light-off values between the different cycles, indication that the catalysts are sensitive to the test conditions even after calcination. The occurring modification had a slight adverse effect for the CO oxidation reaction, while for both HCs and NO the performance increased. Hansen et al., reported that for C_3H_6 oxidation the lower T50 was obtained for Pt particle sizes at around 2 nm, reaction starting after the limiting CO oxidation reaction.[12] Otto et al., reported instead that the dependence on particle size, expressed as rate constant, increases with the increase of particle size.[61] In agreement with the previous studies, the observed difference in performance was ascribed to the occurring surface modifications, and to the varying ratio of coordination sites on the Pt NPs, slightly growing as pointed

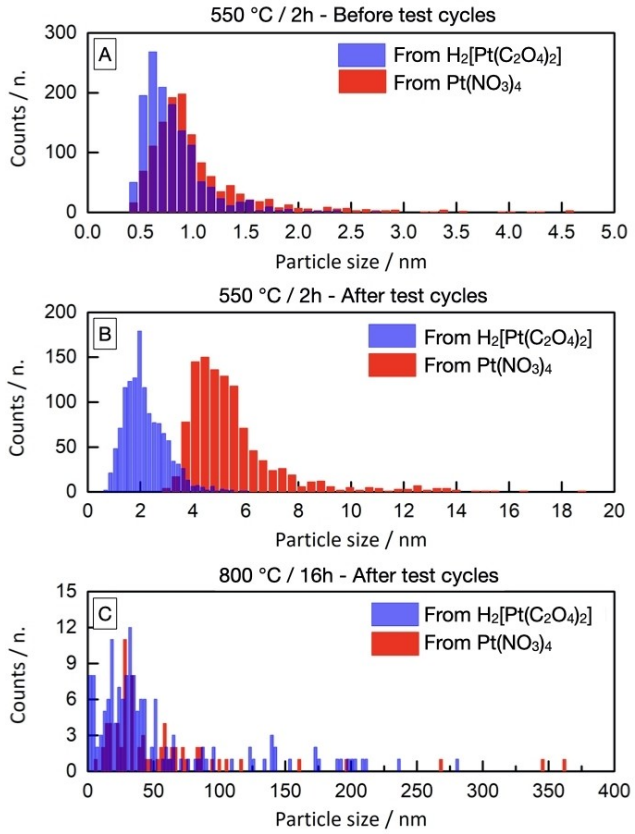

Figure 5. histograms from TEM measurements of samples: A) fresh (550 °C/2 h) before the catalytic test; B) fresh (550 °C/2 h) after the catalytic test C) aged (800 °C/16 h) after catalytic cycles. Red for the reference catalyst prepared from Pt nitrate and blue for the one from bis(oxalato)platinate.

out by TEM.[62] While starting from almost similar average particle sizes prior to the test, the two fresh catalysts behaved quite differently, with higher CO oxidation performance for the Pt bis(oxalate)-based catalyst and slightly better HC and NO performances as well. Interestingly, the reference catalyst outperformed the other in NO oxidation during the first light-off, but then was quickly surpassed by a pronounced increase in NO performance after the second test cycle (Figure 4C). An additional proof of the NPs growth during the testing cycle can be outlined by the small decrease (of about 4% at 130 °C) in the absolute values of catalytic conversion for CO oxidation during the third test cycle (and almost absent in the previous two). Being the total active specific surface area decreased by the increase in particle size, less catalyst is available for the competitive adsorption-desorption reactions in the presence of hydrocarbons. This absolute decrease was observed exactly during the starting light-off for the HCs oxidation (Figure 4). Despite outperforming fresh catalytic performance with respect to the Pt nitrate based catalyst, after the harsh hydrothermal aging, both catalysts showed similar catalytic performance, beside a retained small benefit for the NO oxidation displayed by the oxalate-based catalyst. This is also in agreement with the fact that there is a size dependent relationship[63] of the sintering process occurring at high temperatures (in this study, 800 °C/16 h under hydrothermal conditions), with smaller initial particles expected to be more sensitive to the aging, growing larger, and performing better for the NO oxidation reaction. In fact, TEM analysis in Figure 1, reports bigger particles for the bis(oxalato)platinate sample with respect to the Pt nitrate one after aging. The NO oxidation reaction is more efficient over Pt catalysts with larger particles, since bigger particles are expected to exhibit higher amounts of planar facets, in agreement with the observed results as well as with previous state of the art.[64]

Conclusions

Through an industrially feasible and scalable procedure, a series of catalysts were prepared starting from two different metal precursors. $H_2[Pt(C_2O_4)_2)]$ was used for the first time as an alternative precursor to prepare a highly active DOC catalyst at a kg scale. The effect of synthetic parameters on the resulting final particle size were systematically investigated. The pH of the washcoat was found to impact significantly the catalytic performance for the CO oxidation, likely as a result of the influence on the oligomerisation equilibria of the starting Pt precursor, as observed by UV-Vis. Eventually, the optimised synthesis was scaled-up to produce 2 kg of slurry to coat the cordierite substrate, as described in the experimental part, therefore showing the feasibility of the actual application of the selected halogen-free catalyst. Very small Pt NPs (< 1 nm) with extremely narrow size distribution were synthesised upon decomposition of the Pt salt. Their size evolution under different thermal treatment was followed by TEM and DRIFT and related to the oxidation of CO, C_3H_6 and C_3H_8, as well as NO. The catalyst performance was referenced *vs* a catalyst prepared out of Pt nitrate: surprisingly, the NPs produced from the first precursor resulted more stable against the test conditions experienced during the sequence of three catalytic cycles. A correlation between the higher catalytic performance, particularly for CO oxidation, and the particle size of the samples was pointed out, likely consequence of a better Pt dispersion over the support. The high exothermicity as well as the lower decomposition temperature of this peculiar Pt complex could indeed play a role in this sense, resulting in an improved starting metal dispersion in the catalyst.

Experimental Section

Precursor characterisation

Bis(oxalato)platinate, $H_2[Pt(C_2O_4)_2)]$, was received from Umicore AG & Co. KG as water solution (11.8 wt% Pt), used and characterised without further purifications. Oxalic acid (Merck), nitric acid (65 vol%, Merck) and tetrabutylammonium hydroxide (TEAH, 35 wt% in aqueous solution, Merck) were purchased and used as received. UV-Vis measurements were recorded using an Agilent Cary 60 UV-Vis spectrophotometer. The spectra were collected in the range 200–1000 nm, using quartz cuvettes with 0.1 and 0.01 mm optical paths due to intense absorption. TG-MS coupled with DSC analysis was carried out using a Netzsch STA 449 F3 Jupiter thermogravimeter. The temperature range was between

50 °C and 1000 °C, in a N_2 atmosphere with a heating rate of 10 K/min. ICP-OES measurements were performed using a Varian 725 with radial geometry, mineralizing the samples with a mixture of nitric acid and hydrochloric acid, in a molar ratio of 1:3.

Catalysts preparation and characterisation

γ-alumina was purchased from Sasol (Puralox, 90 m^2/g) and used without further purification. The Pt solutions were deposited onto the γ-alumina through a wet-impregnation deposition. About 2 kg of catalysts were prepared in the following way: the support was previously milled to achieve a size fraction of D50 of 5 μm and a D90 of 15 μm, as measured by light-scattering with a Malvern Mastersizer 2000 instrument. Cordierite substrates were purchased from Corning and the prepared washcoats were coated on the as received material. In the optimization phase, supported powder catalysts (1 wt% Pt) were prepared by wet impregnation of γ-alumina (90 m^2/g) with the $H_2[Pt(C_2O_4)_2]$ solution. Three factors, temperature (25–70 °C), time of impregnation (15–60 min) and Pt metal loading on alumina (1–10 wt%), were changed during the preparation and the resulting Pt concentration on powder was then normalised to 1 wt% with addition of γ-alumina. After drying in air at 120 °C/1 h, the catalysts were degreened (350 °C/4 h), calcined 550 °C/2 h) and eventually aged (800 °C/16 h) to obtain the supported metallic Pt NPs. Transmission electron microscopy (TEM) studies were performed with an Analytical Electronic Philips CM12 operating at an accelerating voltage of 120 kV. At least 1000 counts for each sample were used to calculate the average size. Only for aged samples the counts are based on 100 counts. DRIFT spectra were recorded using a Bruker Optics Vertex 70 Spectrum FTIR spectrometer, equipped with a high-temperature controllable DRIFT cell (Specac). The spectra were recorded in a N_2 flow at 30 °C after pre-treating the samples to H_2 to for 30 min at 200 °C to reduce the Pt NPs. Signal averaging was set with a time of 12 s per spectrum and recorded at a rate of 1 scan/s at a 4 cm^{-1} resolution in a 400–4000 cm^{-1} range. CO chemisorption experiments were performed by using a 10 vol% CO/N_2 gas mixture at 30 °C for 6 min. Cordierite coated catalysts were prepared by wet impregnation of γ-alumina (90 m^2/g) with the $H_2[Pt(C_2O_4)_2]$ solution. pH was eventually varied with both oxalic acid and nitric acid to keep pH below 2 during impregnation (see Supporting Information for further experimental details), and later on set to 6 with tetrabutylammonium hydroxide (TEAH, 35 wt% in aqueous solution).

Catalytic performance measurements

During the optimisation phase, catalytic tests on powders were performed in a fixed-bed quartz reactor (internal diameter 10 mm) using 200 mg of pressed catalysts, finely sieved and collected with size between 500–700 μm and mixed with 400 mg of γ-alumina of the same grain size. Space velocity was of approximately 50 1/h and the temperature ramp employed for all the analysis was 1 K/min from 75 °C to 500 °C. The reactant mixture encompassed 350 ppm CO, 5 vol.% H_2O, 6 vol.% O_2, 10.7 vol.% CO_2 and N_2 as carrier gas. Exit gas composition was measured using a Varian CP-4900 Micro-GC gas chromatograph (GC), with a TCD detector.

For catalytic tests on cordierite coated catalysts, 2 kg washcoats were prepared for each catalyst and monoliths (length: 7.62 cm, diameter: 2.54 cm, 400 cpsi, 0.1016 mm wall thickness, final Pt loading of 90 g/ft^3) were used for all experiments. Monoliths were wrapped with insulation tape and placed in a stainless steel tubular reactor ensuring no gas bypass. The test bench encompassed a gas mixing unit and pipes, a gas pre-heater, the main reactor and the analyser module. Mass flow controllers were used to control and monitor the flow rate of each pollutant. Chemi-luminescence detector (CLD) analyser was used to reveal the NO and NO_x, a flame ionization detector (FID) was employed to detect hydrocarbons, a paramagnetic method (MLT) was utilized to monitor O_2, while CO and CO_2 were analysed applying a non-dispersive infrared sensor (NDIR).[65] All catalytic test on coated catalysts cycles were repeated twice six month apart, showing no differences in absolute values and trends.

As pre-treatment, the catalysts were exposed to the reaction mixture at 50 °C for 15 min. Three light-off experiments were performed, with space velocity of approximately 37500 1/h. The temperature ramp employed for all the catalytic tests was 10 K/min from 75 °C to 500 °C.

Gas composition for all catalytic tests consisted of 350 ppm CO, 60 ppm C_3H_6, 30 ppm C_3H_8, 270 ppm NO, 115 ppm H_2, 10.7% CO_2, 6.0% O_2, 5.0% H_2O balanced with N_2.

Additional Information

The authors have cited additional references within the Supporting Information.[66–70]

Acknowledgements

Umicore AG & Co. KG is gratefully acknowledged for financial support and funding of a PhD fellowship to F.S. The authors would like to express their gratitude to Dr. Wan for his support with the TG-MS and DRIFT spectroscopy analyses. Mrs Kerstin Neuhan is also kindly acknowledged for the support in the preparation of the catalysts and same is Dr. Keitl, for the fruitful discussions. S.G. warmly thanks DFG and the SFB project CRC 1441 "TrackAct" for the provision of a Mercator Fellow position at KIT and the University of Padova.

Conflict of Interests

The authors declare no conflict of interest.

Data Availability Statement

The data that support the findings of this study are available from the corresponding author upon reasonable request.

Keywords: Platinum · Environmental pollutants · Heterogeneous catalyst · Diesel Oxidation Catalyst · Nanoparticles

[1] A. K. Datye, M. Votsmeier, *Nat. Mater.* **2021**, *20*, 1049–1059.
[2] M. V. Twigg, *Catal. Today* **2011**, *163*, 33–41.
[3] M. V. Twigg, *Appl. Catal. B* **2007**, *70*, 2–15.
[4] A. V. Karre, R. K. Garlapalli, A. Jena, N. Tripathi, *Catal. Commun.* **2023**, *179*, 106682.
[5] R. M. Heck, R. J. Farrauto, *Appl. Catal. A* **2001**, *221*, 443–457.
[6] G. Ertl, H. Knözinger, F. Schüth, J. Weitkamp, *Handbook of Heterogeneous Catalysis*, Wiley-VCH Verlag GmbH & Co. KGaA, Weinheim, Germany, **2008**.

[7] P. Granger, V. I. Parvulescu, *Chem. Rev.* **2011**, *111*, 3155–3207.
[8] R. A. Van Santen, *Acc. Chem. Res.* **2009**, *42*, 57–66.
[9] A. Y. Stakheev, D. A. Bokarev, I. P. Prosvirin, V. I. Bukhtiyarov, in *Adv. Nanomater. Catal. Energy*, Elsevier, **2019**, pp. 295–320.
[10] A. Russell, W. S. Epling, *Catal. Rev.* **2011**, *53*, 337–423.
[11] S. B. Simonsen, I. Chorkendorff, S. Dahl, M. Skoglundh, K. Meinander, T. N. Jensen, J. V. Lauritsen, S. Helveg, *J. Phys. Chem. C* **2012**, *116*, 5646–5653.
[12] T. K. Hansen, M. Høj, B. B. Hansen, T. V. W. Janssens, A. D. Jensen, *Top. Catal.* **2017**, *60*, 1333–1344.
[13] T. W. Hansen, A. T. DeLaRiva, S. R. Challa, A. K. Datye, *Acc. Chem. Res.* **2013**, *46*, 1720–1730.
[14] C. T. Campbell, Z. Mao, *ACS Catal.* **2017**, *7*, 8460–8466.
[15] M. J. Hazlett, W. S. Epling, *Catal. Today* **2016**, *267*, 157–166.
[16] T. W. Van Deelen, C. Hernández Mejía, K. P. De Jong, *Nat. Catal.* **2019**, *2*, 955–970.
[17] Y. Li, Y. Zhang, K. Qian, W. Huang, *ACS Catal.* **2022**, *12*, 1268–1287.
[18] C. Carrillo, A. DeLaRiva, H. Xiong, E. J. Peterson, M. N. Spilde, D. Kunwar, R. S. Goeke, M. Wiebenga, S. H. Oh, G. Qi, S. R. Challa, A. K. Datye, *Appl. Catal. B* **2017**, *218*, 581–590.
[19] P. Anguita, J. M. García-Vargas, F. Gaillard, E. Iojoiu, S. Gil, A. Giroir-Fendler, *Chem. Eng. J.* **2018**, *352*, 333–342.
[20] Z. Zhang, J. Tian, J. Li, C. Cao, S. Wang, J. Lv, W. Zheng, D. Tan, *Fuel Process. Technol.* **2022**, *233*, 107317.
[21] C. H. Bartholomew, *Appl. Catal. A* **2001**, *212*, 17–60.
[22] A. V. Nartova, L. M. Kovtunova, Y. V. Larichev, A. K. Khudorozhkov, A. N. Bobrovskaya, G. V. Shterk, V. I. Bukhtiyarov, *Mendeleev Commun.* **2017**, *27*, 70–71.
[23] M. M. Azis, X. Auvray, L. Olsson, D. Creaser, *Appl. Catal. B* **2015**, *179*, 542–550.
[24] N. Batalha, L. Pinard, S. Morisset, J. L. Lemberton, Y. Pouilloux, M. Guisnet, F. Lemos, F. R. Ribeiro, *React. Kinet. Mech. Catal.* **2012**, *107*, 285–294.
[25] B. Kucharczyk, B. Szczygieł, J. Chęcmanowski, *Open Chemistry* **2017**, *15*, 182–188.
[26] L. Geng, J. Gong, G. Qiao, S. Ye, J. Zheng, N. Zhang, B. Chen, *ACS Omega* **2019**, *4*, 12598–12605.
[27] M. J. Hazlett, W. S. Epling, *Catal. Today* **2021**, *360*, 401–410.
[28] B. Zhu, F. Letellier, J. Blanchard, K. Fajerwerg, C. Louis, D. Guillaume, D. Uzio, M. Breysse, **2006**, pp. 449–456.
[29] Z. Vít, D. Gulková, L. Kaluža, M. Boaro, *Appl. Catal. B* **2014**, *146*, 213–220.
[30] C. Zhang, S. N. Oliaee, S. Y. Hwang, X. Kong, Z. Peng, *Nano Lett.* **2016**, *16*, 164–169.
[31] Z. Abdelouahab-Reddam, R. El Mail, F. Coloma, A. Sepúlveda-Escribano, *Catal. Today* **2015**, *249*, 109–116.
[32] R. M. Ravenelle, F. Z. Diallo, J. C. Crittenden, C. Sievers, *ChemCatChem* **2012**, *4*, 492–494.
[33] M. Argyle, C. Bartholomew, *Catalysts* **2015**, *5*, 145–269.
[34] M. Paulis, H. Peyrard, M. Montes, *J. Catal.* **2001**, *199*, 30–40.
[35] E. Marceau, H. Lauron-Pernot, M. Che, *J. Catal.* **2001**, *197*, 394–405.
[36] J. W. Döbereiner, *Poggendorffs Ann. Phys.* **1833**, *28*, 180.
[37] H. G. Soderbaum, *Bull. Soc. Chim.* **1886**, *45*, 188.
[38] H. G. Soderbaum, *Chem. Ber.* **1888**, *21*, 576 C.
[39] K. Krogmann, P. Dodel, *Chem. Ber.* **1966**, *188*, 239–247.
[40] K. Krogmann, P. Dodel, *Chem. Ber.* **1966**, *99*, 3408–3418.
[41] X. Fu, Y. Wang, N. Wu, L. Gui, Y. Tang, *Langmuir* **2002**, *18*, 4619–4624.
[42] S. U. Dunham, E. H. Abbott, *Inorg. Chim. Acta* **2000**, *297*, 72–78.
[43] A. E. Underhill, D. M. Watkins, J. M. Williams, K. Carneiro, in *Ext. Linear Chain Compd.*, Springer US, Boston, MA, **1982**, pp. 119–156.
[44] B. M. Anderson, S. K. Hurst, *Eur. J. Inorg. Chem.* **2009**, *2009*, 3041–3054.
[45] C. Yamamoto, H. Nishikawa, M. Nihei, T. Shiga, M. Hedo, Y. Uwatoko, H. Sawa, H. Kitagawa, Y. Taguchi, Y. Iwasa, H. Oshio, *Inorg. Chem.* **2006**, *45*, 10270–10276.
[46] B. J. Keller, S. K. Hurst, S. O. Dunham, L. Spangler, E. H. Abbott, E. S. Peterson, *Inorg. Chim. Acta* **2004**, *357*, 853–858.
[47] K. Hauff, U. Tuttlies, G. Eigenberger, U. Nieken, *Appl. Catal. B* **2012**, *123–124*, 107–116.
[48] D. Dou, D. Liu, W. B. Williamson, K. C. Kharas, H. J. Robota, *Appl. Catal. B* **2001**, *30*, 11–24.
[49] C. D. Zeinalipour-Yazdi, D. J. Willock, L. Thomas, K. Wilson, A. F. Lee, *Surf. Sci.* **2016**, *646*, 210–220.
[50] X. Wang, P. Sonström, D. Arndt, J. Stöver, V. Zielasek, H. Borchert, K. Thiel, K. Al-Shamery, M. Bäumer, *J. Catal.* **2011**, *278*, 143–152.
[51] F. Illas, S. Zurita, A. M. Márquez, J. Rubio, *Surf. Sci.* **1997**, *376*, 279–296.
[52] A. Garnier, S. Sall, F. Garin, M. J. Chetcuti, C. Petit, *J. Mol. Catal. A* **2013**, *373*, 127–134.
[53] M. Casapu, A. Fischer, A. M. Gänzler, R. Popescu, M. Crone, D. Gerthsen, M. Türk, J. D. Grunwaldt, *ACS Catal.* **2017**, *7*, 343–355.
[54] L. Li, A. H. Larsen, N. A. Romero, V. A. Morozov, C. Glinsvad, F. Abild-pedersen, J. Greeley, K. W. Jacobsen, J. K. Nørskov, *J. Phys. Chem. Lett.* **2013**, *4*, 222–226.
[55] E. K. Gibson, E. M. Crabb, D. Gianolio, A. E. Russell, D. Thompsett, P. P. Wells, *Catal. Struct. React.* **2017**, *3*, 5–12.
[56] A. Winkler, D. Ferri, M. Aguirre, *Appl. Catal. B* **2009**, *93*, 177–184.
[57] İ. A. Reşitoğlu, K. Altinişik, A. Keskin, *Clean Technol. Environ. Policy* **2015**, *17*, 15–27.
[58] C. Yin, F. R. Negreiros, G. Barcaro, A. Beniya, L. Sementa, E. C. Tyo, S. Bartling, K.-H. Meiwes-Broer, S. Seifert, H. Hirata, N. Isomura, S. Nigam, C. Majumder, Y. Watanabe, A. Fortunelli, S. Vajda, *J. Mater. Chem. A* **2017**, *5*, 4923–4931.
[59] A. M. Gänzler, M. Casapu, A. Boubnov, O. Müller, S. Conrad, H. Lichtenberg, R. Frahm, J. D. Grunwaldt, *J. Catal.* **2015**, *328*, 216–224.
[60] Y. Wang, C. Pei, X. Wang, G. Sun, Z.-J. Zhao, J. Gong, *Fundam. Res.* **2022**, *In press*, DOI 10.1016/j.fmre.2022.08.020.
[61] K. Otto, J. M. Andino, C. L. Parks, *J. Catal.* **1991**, *131*, 243–251.
[62] F. J. Gracia, L. Bollmann, E. E. Wolf, J. T. Miller, A. J. Kropf, *J. Catal.* **2003**, *220*, 382–391.
[63] C. T. Campbell, *Science* **2002**, *298*, 811–814.
[64] A. Boubnov, S. Dahl, E. Johnson, A. P. Molina, S. B. Simonsen, F. M. Cano, S. Helveg, L. J. Lemus-Yegres, J.-D. Grunwaldt, *Appl. Catal. B* **2012**, *126*, 315–325.
[65] M. Herrmann, R. E. Hayes, M. Votsmeier, *Appl. Catal. B* **2018**, *220*, 446–461.
[66] K. Nakamoto, *Infrared and Raman Spectra of Inorganic and Coordination Compounds*, John Wiley & Sons, Inc., Hoboken, NJ, USA, **2008**.
[67] K. D. Dobson, A. J. McQuillan, *Spectrochim. Acta Part A* **1999**, *55*, 1395–1405.
[68] S. J. Hug, D. Bahnemann, *J. Electron Spectrosc. Relat. Phenom.* **2006**, *150*, 208–219.
[69] S. B. Johnson, T. H. Yoon, A. J. Slowey, G. E. Brown, *Langmuir* **2004**, *20*, 11480–11492.
[70] N. M. Martin, J. Nilsson, M. Skoglundh, E. C. Adams, X. Wang, G. Smedler, A. Raj, D. Thompsett, G. Agostini, S. Carlson, K. Norén, P.-A. Carlsson, *Catal. Struct. React.* **2017**, *3*, 24–32.

Manuscript received: August 16, 2023
Revised manuscript received: October 20, 2023
Accepted manuscript online: November 7, 2023
Version of record online: December 6, 2023